

# Hybrid Zero Dynamics based Multiple Shooting Optimization with Applications to Robotic Walking

Ayonga Hereid<sup>1</sup>, Christian M. Hubicki<sup>2</sup>, Eric A. Cousineau<sup>1</sup>, Jonathan W. Hurst<sup>2</sup> and Aaron D. Ames<sup>1</sup>

**Abstract**—Hybrid zero dynamics (HZD) has emerged as a popular framework for the stable control of bipedal robotic gaits, but typically designing a gait’s virtual constraints is a slow and undependable optimization process. To expedite and boost the reliability of HZD gait generation, we borrow methods from trajectory optimization to formulate a smoother and more linear optimization problem. We present a multiple-shooting formulation for the optimization of virtual constraints, combining the stability-friendly properties of HZD with an optimization-conducive problem formulation. To showcase the implications of this recipe for improving gait generation, we use the same process to generate periodic planar walking gaits on two different robot models, and in one case, demonstrate stable walking on the hardware prototype, DURUS-R.

## I. INTRODUCTION

*Hybrid zero dynamics* (HZD) [22] is a framework that has been at the core of many successful bipedal robot control implementations [7], [20], [23], especially in the analytically tricky domain of underactuated machines. By properly designing a set of virtual constraints to enforce via feedback control, hybrid invariance can be achieved, assuring stability despite periodic leg impacts and support changes. This key task of finding an appropriate set of virtual constraints is typically relegated to an optimization. However, given the nonlinearity of bipedal robot dynamics, it can be difficult to achieve reliable convergence via this optimization and often relies upon expert users to seed it. By borrowing tools from the trajectory optimization community, we claim that a thoughtful recipe for problem formulation can make virtual constraint optimization a sufficiently reliable, and therefore automatable, process.

The most intuitive approach to formulating optimal control problems is arguably the direct shooting method. A subset of direct optimization methods [18], the direct shooting method parameterizes the control inputs with certain basis functions, either linear [17] or nonlinear [1], simulates the dynamics via a single time-marching numerical integration, and then evaluates the objective and all constraints. Such “single shooting” is the most prevalent formulation for optimizing virtual constraints in the context of HZD. This approach of optimizing only parameters and boundary state values reflects an instinctive desire to reduce the number of design

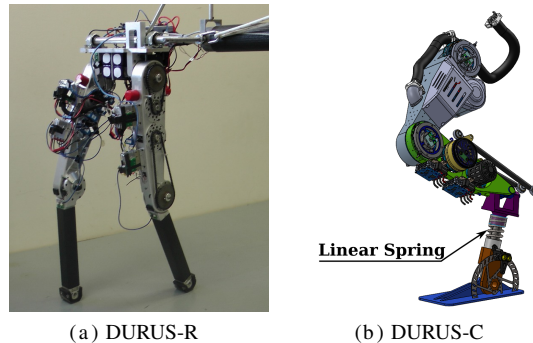


Fig. 1: DURUS series prototype robots.

variables for the optimization. Intuitively, one might assume that such minimization of the nonlinear programming problems (NLPs) dimensionality would be an advisable practice for maximizing an optimization’s speed and reliability.

However, not all design variables are equally complicated for an NLP solver to navigate, a fact which *multiple-shooting* methods exploit. For common NLP-solving methods like interior point and sequential quadratic programming, convergence is more reliable when the objectives and constraints are smooth and relatively linear. In a single shooting formulation, a change to a parameter or boundary state value can have a very nonlinear effect on the final state, after integrating nonlinear dynamics over non-trivial time scales. This type of nonlinearity can cause an optimizer to fail to converge or be uncertain if it has found a solution.

Multiple shooting is designed to ameliorate this manner of nonlinearity [6], [9]; specifically it splits each discretization segment of the input tape into its own small trajectory optimization problem, each with its own set of control inputs and of initial state conditions, but a shorter horizon for integration. With finer discretization, this integration horizon approaches zero, rendering the relationship between control inputs and the post-integration state increasingly linear. This property has made multiple shooting methods (and conceptually similar direct collocation methods [21]) fast and reliable for planning gaits for high-dimensional robots.

The goal of this paper is to provide a general optimization formulation for the optimal control of multi-domain hybrid systems that effectively incorporates and combines the dimension reduction and formal establishment of stability enjoyed from HZD and optimization advantages of multiple shooting methods. Virtual constraints parameterized by *canonical walking functions* are used to construct the zero dynamics for the multi-domain hybrid control system,

This research is supported by SRI International.

<sup>1</sup>A. Hereid, E. A. Cousineau and A. D. Ames are with the Department of Mechanical Engineering, Texas A&M University, College Station, TX 77843, e-mail: {ayonga, eacousineau, aames}@tamu.edu

<sup>2</sup>J. W. Hurst and C. M. Hubicki are with the Department of Mechanical, Industrial and Manufacturing Engineering, Oregon State University, Corvallis, OR 97330, e-mail: hubickic@onid.orst.edu, jonathan.hurst@oregonstate.edu

then the proposed HZD based multiple shooting optimization method is applied to generate optimal trajectories for the system. We then apply the formulation to two underactuated bipedal robots, DURUS-R and DURUS-C shown in Fig. 1, to demonstrate the effectiveness and reliability of this method.

## II. OVERVIEW OF CURRENT APPROACHES

We start with a brief overview of the prevalent HZD based optimization framework. Most of these optimization problems use direct shooting methods (heretofore referred to as *single shooting* methods<sup>1</sup>) which are often unlikely to converge or are very sensitive to initial guesses. On the other hand, direct multiple shooting methods (*multiple shooting* for brevity) are designed to mitigate this NLP nonlinearity, without approximation, by discretizing both control inputs and states.

**HZD based Optimization.** As discussed in [22], [15], with a set of properly designed virtual constraints, the full order bipedal robot dynamics can be projected to a reduced dimensional dynamics, called *zero dynamics*. The main goal of HZD based optimization problems is to obtain a parameter set for virtual constraints that results in a hybrid invariant zero dynamics. Most optimization problems for hybrid zero dynamics are formulated to find the optimal parameter set  $\alpha^*$  and the fixed point  $z^*$  of the zero dynamics:

$$\begin{aligned} & \underset{\alpha, z^-}{\operatorname{argmin}} J(z(t), \alpha) & (1) \\ \text{s.t. } & h(z(t), \alpha) \leq 0, & \text{(path constraints)} \\ & g(z^-) = 0, & \text{(guard constraints)} \end{aligned}$$

where  $J_v(z(t), \alpha)$  is the cost function with  $z(t)$  the solution of zero dynamics with initial condition determined from the fixed point  $z^-$ . Moreover, an additional constraint is also imposed to ensure hybrid invariance of the zero dynamics. The path constraints and the objective function are evaluated by integrating the zero dynamics with the given initial conditions. Though this single-shooting formulation has fewer optimization variables, any small changes in the optimization variables will propagate (in ways that are possibly highly nonlinear) as the dynamics is integrated over the full course of one step.

**Multiple Shooting Optimization.** Instead of using parameterized controllers like an HZD based optimization, a multiple shooting approach discretizes both control inputs and states, which gives the optimizer the ability to more directly shape the evolution of the state. Here, we consider a typical optimal control problem that finds the control input  $u(t)$  of a control system determined by the ODE

$$\dot{x}(t) = f(x(t), u(t)), \quad t_0 \leq t \leq t_f, \quad (2)$$

<sup>1</sup>In a detailed survey paper, [18] makes a clear conceptual distinction between indirect methods (such as indirect shooting, indirect multiple shooting) and direct methods (e.g. the direct shooting and direct multiple shooting methods addressed in this paper). In practice, direct methods are significantly more common in legged robot control than indirect methods. So for ease of communication, we both drop the “direct” adjective and rename “direct shooting” to “single shooting” [14] to verbally distinguish it from “multiple shooting.”

while minimizing the objective function  $J(x(t), u(t))$ . The integration time scale  $[t_n, t_f]$  is often discretized as

$$t_0 = t_0 < t_1 < t_2 \cdots < t_n = t_f, \quad n \geq 1, \quad (3)$$

and the multiple shooting optimization is formulated as:

$$\begin{aligned} & \underset{w}{\operatorname{argmin}} J(w) & (4) \\ \text{s.t. } & x_{i+1} - x(x_i, u_i; t_{i+1}) = 0, & \text{(continuity condition)} \\ & h(x_i, u_i) \leq 0, & \text{(path constraints)} \\ & g(x_n, u_n, t_f) = 0, & \text{(terminal constraints)} \end{aligned}$$

where  $w = (x_1, u_1, \dots, x_n, u_n, t_f)$  is a vector of optimization variables with  $x_i = x(t_i)$  and  $u_i = u(t_i)$ , and  $x(x_i, u_i; t_{i+1})$  is the solution of system (2) at  $t_{i+1}$  starting from  $x_i$  with the control input  $u_i$ . Though this formulation makes the convergence more reliable by discretization, it lacks a necessary feedback relationship between system states and control inputs.

## III. HZD BASED MULTIPLE SHOOTING OPTIMIZATION

In this section, we present a combined approach, *hybrid zero dynamics based multiple shooting optimization*, which commingles the underlying advantages of multiple shooting methods with zero dynamics. To begin with, we introduce the formal definition and theory of the *multi-domain hybrid control system* and the *hybrid zero dynamics*.

### A. Hybrid Control System

Hybrid systems are systems that consist of both smooth, continuous dynamics and discrete dynamics, and thus have a wide range of applications to various types of physical systems [11]. A typical example of these applications is bipedal robotic walking. In the case of multi-contact bipedal locomotion, we consider a *multi-domain hybrid control system*, which is given as a *tuple* [4], [19]:

$$\mathcal{HC} = (\Gamma, \mathcal{D}, \mathcal{U}, S, \Delta, FG), \quad (5)$$

where  $\Gamma = \{V, E\}$  is a directed cycle with vertices  $V$  and edges  $E$ ,  $\mathcal{D} = \{\mathcal{D}_v\}_{v \in V}$  is a set of domains of continuous dynamics,  $\mathcal{U} = \{\mathcal{U}_v\}_{v \in V}$  is a set of admissible controls,  $S = \{S_e \subset \mathcal{D}_v\}_{e \in E}$  is a set of *guards* or *switching surfaces*,  $\Delta = \{\Delta_e\}_{e \in E}$  is a set of smooth *reset maps* that maps system states  $x \in S_e$  to the next domain  $\mathcal{D}_{v^+}$  in the cycle, and  $FG = \{FG_v\}_{v \in V}$  is a set of control systems defined on  $\mathcal{D}_v$ . Given the configuration space  $\mathcal{Q}$ , let  $q \in \mathcal{Q}$  be the generalized coordinates of a robot model. The equation of motion (EOM) for a domain  $\mathcal{D}_v$  is determined by the classical Euler-Lagrange equation and holonomic constraints [10]:

$$D(q)\ddot{q} + H(q, \dot{q}) = B_v u_v + J_v^T(q) F_v, \quad (6)$$

$$J_v(q)\ddot{q} + \dot{J}_v(q, \dot{q})\dot{q} = 0, \quad (7)$$

where  $D(q)$  is the inertia matrix,  $H(q, \dot{q})$  is the vector containing the Coriolis and gravity term,  $B_v$  is the actuator distribution matrix,  $J_v(q)$  is the Jacobian of the holonomic

constraints  $\eta_v(q)$ , and  $F_v$  is a *wrench* containing the constraints' external forces and/or moments.  $F_v$  can be explicitly solved as a function of system states and torques by combining (6) and (7). However, in this paper, we consider  $F_v$  as a part of the control inputs that satisfy (6) and (7) simultaneously. Then let

$$\bar{B}_v(q) = [B_v \quad J_v^T(q)], \quad \bar{u}_v = [u_v \quad F_v]^T, \quad (8)$$

to yield equations of motion as the affine control system

$$\dot{x} = f(x) + g_v(x)\bar{u}_v \quad (9)$$

from (6) with  $x = (q, \dot{q})$  the system states, where

$$f(x) = \begin{bmatrix} \dot{q} \\ -D^{-1}(q)H(q, \dot{q}) \end{bmatrix}, \quad g_v(x) = \begin{bmatrix} \mathbf{0} \\ D^{-1}(q)\bar{B}_v(q) \end{bmatrix}.$$

The discrete dynamics is determined by the changes in the contact points of the system. For bipedal robots, the configuration of the system are assumed to be invariant through impact, but the velocities of robot joints are determined through the impact equation by imposing the holonomic constraints of the subsequent domain. Given pre-impact states  $(q^-, \dot{q}^-)$ , the post impact states  $(q^+, \dot{q}^+)$  are computed by the reset map  $\Delta_e$ :

$$\begin{bmatrix} q^+ \\ \dot{q}^+ \end{bmatrix} = \begin{bmatrix} \mathcal{R}q^- \\ \mathcal{R}\Delta(q^-)\dot{q}^- \end{bmatrix}, \quad (10)$$

where  $\mathcal{R}$  is the relabeling matrix if there is a coordinate change due to switching of stance and non-stance legs, and  $\Delta(q^-)\dot{q}^-$  is the plastic impact equation [13], [10].

Any applicable state-based feedback controllers,  $\bar{u}_v$ , that have been applied on the control system,  $FG_v$ , yield closed-loop dynamics. We define the resulting autonomous hybrid system as a *multi-domain hybrid system*:

$$\mathcal{H} = (\Gamma, \mathcal{D}, S, \Delta, F), \quad (11)$$

where  $F$  is a set of smooth vector fields on  $\mathcal{D}$  with  $\dot{x} = f_v(x)$ .

### B. Virtual Constraints and Hybrid Zero Dynamics

Analogous to holonomic constraints, virtual constraints are defined as functions of the robot configuration to describe the behavior of bipedal walking, such as swinging the non-stance leg forward, keeping the torso straight, etc. The term ‘‘virtual’’ comes from the fact that these constraints are enforced through feedback control instead of through physical constraints. Let  $y_v^a(q)$  be functions of the robot configuration to be controlled, and  $y_v^d(\tau(q), \alpha)$  be the corresponding desired behaviors parameterized by  $\alpha$ , where  $\tau(q)$  is a strictly monotonic function of  $q$  that parameterizes time. The virtual constraints are then defined on the domain  $\mathcal{D}_v$  as

$$y_v(q) = y_v^a(q) - y_v^d(\tau(q), \alpha) \equiv 0. \quad (12)$$

Note that we use the *canonical walking function* (CWF) for desired trajectories in this paper. We refer the readers to [1], [2] for the details of CWF within the context of Human-Inspired Control.

Combining holonomic constraints and virtual constraints together, and differentiating  $(y_v(q), \eta_v(q))$  twice yields

$$\begin{bmatrix} \ddot{y}_v(q, \dot{q}) \\ \ddot{\eta}_v(q, \dot{q}) \end{bmatrix} = \underbrace{\begin{bmatrix} L_{g_v} L_f y_v(q, \dot{q}) \\ L_{g_v} L_f \eta_v(q, \dot{q}) \end{bmatrix}}_{\mathcal{A}_v} + \underbrace{\begin{bmatrix} L_f^2 y_v(q, \dot{q}) \\ L_f^2 \eta_v(q, \dot{q}) \end{bmatrix}}_{(L_f^2)_v} \bar{u}_v, \quad (13)$$

where  $L$  represents the Lie derivative. If  $y_v(q)$  has the same dimension as the control input  $u_v$  and the Jacobian of  $(y_v(q), \eta_v(q))$  w.r.t.  $q$  has a full rank, then the *decoupling matrix*,  $\mathcal{A}_v$ , is invertible. An input-output feedback controller,

$$\bar{u}_v(x) = -\mathcal{A}_v^{-1}((L_f^2)_v + \bar{\mu}_v), \quad (14)$$

with  $\bar{\mu}_v = [-2\varepsilon L_f y_v - \varepsilon^2 y_v; \mathbf{0}]$  for  $\varepsilon > 0$ , drives the output  $y(q) \rightarrow 0$  exponentially and guarantees the holonomic constraints in (7) are satisfied simultaneously. In addition, the control law renders the *zero dynamics* submanifold

$$\mathbf{Z}_v = \{x \in \mathcal{D}_v | y_v(q) = 0, L_f y_v(q, \dot{q}) = 0\} \quad (15)$$

invariant over the continuous dynamics of the domain. However, it is not necessarily invariant through discrete dynamics. Therefore, a submanifold  $\mathbf{Z}_v$  is impact invariant if

$$\Delta_e(x) \in \mathbf{Z}_{v^+}, \quad \forall x \in S_e \cap \mathbf{Z}_v. \quad (16)$$

A manifold  $\mathbf{Z} = \bigcup_{v \in V} \mathbf{Z}_v$  is called hybrid invariant if it is invariant over all domains of continuous dynamics and impact invariant through all discrete dynamics, i.e., solutions that start in  $\mathbf{Z}$  remain in  $\mathbf{Z}$ , even after impulse effects. If a feedback control law renders  $\mathbf{Z}$  hybrid invariant, then we say that the multi-domain hybrid control system has a *hybrid zero dynamics* (HZD),  $\mathcal{H}|_{\mathbf{Z}}$ .

In fact, the restricted reduced dimensional dynamics are independent of control effort  $\varepsilon$  and  $\bar{u}_v$ . To determine the dynamics equations of zero dynamics, let  $z_v = \theta_v(q)$  be a real-valued function representing the local coordinates of the zero dynamics  $\mathbf{Z}_v$ . Then

$$\Phi_v(q) := [y_v(q) \quad \eta_v(q) \quad \theta_v(q)]^T : \mathcal{Q} \rightarrow \mathbb{R}^n \quad (17)$$

is a diffeomorphism onto its image and there exists at least one point where both the virtual and holonomic constraints vanish, i.e., *zero dynamics* manifold. Let

$$\xi_{1,v} = \theta_v(q), \quad \xi_{2,v} = \gamma_v(q, \dot{q}) := \gamma_v^0(q)\dot{q}, \quad (18)$$

be the states of the zero dynamics, where  $\gamma_v^0(q) = \ell_v(q)D(q)$  with  $\ell_v(q) \in \text{Null}(\bar{B}_v)$ . It is easy to verify that  $L_{g_v} \gamma_v(q, \dot{q}) = 0$ . Then, the EOM of the zero dynamics can be expressed explicitly:

$$\dot{z}_v = \begin{bmatrix} \dot{\xi}_{1,v} \\ \dot{\xi}_{2,v} \end{bmatrix} = \begin{bmatrix} L_f \theta_v(q, \dot{q}) \\ L_f \gamma_v(q, \dot{q}) \end{bmatrix} := q_v(z_v, \alpha_v), \quad (19)$$

which is independent of the control torque input  $\bar{u}$ . When the system evolves on the *zero dynamics* manifold, the full order states can be reconstructed as follows:

$$q = \Phi_v^{-1}(0, 0, \xi_{1,v}), \quad \dot{q} = \begin{bmatrix} \frac{\partial y_v(q)}{\partial q} \\ J_v(q) \\ \gamma_v^0(q) \end{bmatrix}^{-1} \begin{bmatrix} 0 \\ 0 \\ \xi_{2,v} \end{bmatrix}. \quad (20)$$

That is, the zero dynamics (19) determines the behavior of the full order system. It is shown in [15], [3] that if the system has HZD and there exists a hybrid periodic orbit,  $\mathcal{O}|_{\mathbf{z}}$ , of  $\mathcal{H}|_{\mathbf{z}}$ , as shown in Fig. 2(a), then the full order system has a hybrid periodic orbit  $\mathcal{O}$ .

### C. HZD based Multiple Shooting Optimization

Based on the formal construction of *hybrid zero dynamics*, we present our main result of the paper – HZD based multiple shooting optimization.

Let  $T_v^I \in \mathbb{R}$  be the time where the system hits the corresponding guard of the domain. We uniformly divide a continuous domain into  $n$  shooting grids, i.e.,

$$0 = t_0 < t_1 < t_2 \cdots < t_n = T_v^I, \quad n \geq 1. \quad (21)$$

with an abstract example shown in Fig. 2(b). For each shooting grid  $s_i$  defined on  $t \in [t_i, t_{i+1}] \subset \mathbb{R}$ , let the initial condition  $z_v^i$  and control parameters  $\alpha_v^i$  of the zero dynamics be the optimization variables. Hence the solution of the zero dynamics on shooting grids can be represented as *initial value problems* defined below:

$$\dot{z}_v = q_v(z_v, \alpha_v^i), \quad z_v(t_i) = z_v^i, \quad t \in [t_i, t_{i+1}], \quad (22)$$

where  $i \in \{0, 1, \dots, n-1\}$ .

Combining both HZD based optimization and multiple shooting optimizations, we propose a *HZD based multiple shooting* optimization problem for a multi-domain hybrid system:

$$\underset{w}{\operatorname{argmin}} \sum_{v \in V} J_v(w_v) \quad (23)$$

$$\text{s.t. } z_v(z_v^i, \alpha_v^i; t_{i+1}) - z_v^{i+1} = 0, \quad i \in [0, n-1], \quad (C1)$$

$$\alpha_v^i - \alpha_v^{i+1} = 0, \quad i \in [0, n-1], \quad (C2)$$

$$h_v(z_v^i, \alpha_v^i) \leq 0, \quad i \in [0, n], \quad (C3)$$

$$g_v(z_v^n, \alpha_v^n) = 0, \quad (C4)$$

$$\Delta_e|_{S_e \cap \mathbf{Z}_v}(z_v^n) \in \mathbf{Z}_{v^+}, \quad v, v^+ \in V, e \in E, \quad (C5)$$

$$\alpha_v^n - \alpha_{v^+}^0 = 0, \quad v, v^+ \in V, \quad (C6)$$

where  $w$  is the combination of optimization variables defined on each domain, i.e.,  $w = \bigcup_{v \in V} w_v$  with  $w_v = (z_v^0, \alpha_v^0, \dots, z_v^n, \alpha_v^n, T_v^I)$ , and  $z_v(z_v^i, \alpha_v^i; t_{i+1})$  is the solution of system (22) at  $t_{i+1}$ . Constraints (C1) and (C2) establish both state continuity and parameter equality between two connected shooting grids, constraints (C3) and (C4) are the physical path and terminal conditions, constraints (C5) imposes the hybrid invariance of the zero dynamics at impacts, and constraints (C6) enforces equality of parameters between two domains.

## IV. APPLICATIONS TO BIPEDAL ROBOTS

In this section, we utilize the HZD based multiple shooting optimization method on two different underactuated bipedal robots, DURUS-C and DURUS-R, to generate stable periodic walking gaits on both platforms. DURUS-C and DURUS-R are the prototype DURUS series robots designed by SRI International, shown in Fig. 1, where ‘R’ represents rigid legs, and ‘C’ represents compliant legs.

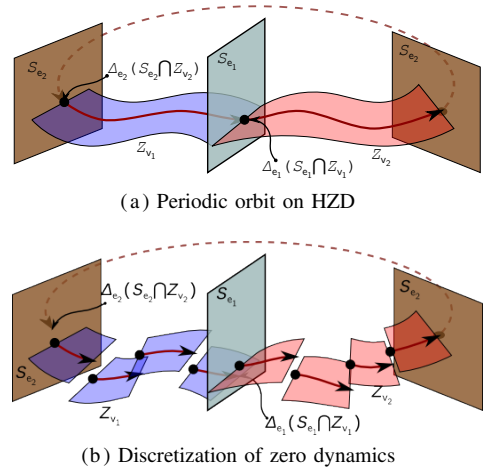


Fig. 2: (a) HZD periodic orbit of a two-domain hybrid control system. (b) A discretization of the hybrid system for integration with multiple-shooting optimization methods.

### A. DURUS-R Model and Optimization

DURUS-R is a planar five-link robot with underactuated point feet; it utilizes advanced mechanical and electrical designs including novel cycloid drive gearing, high-current motor drivers, etc. The robot configuration  $q = (p_x, p_z, q_{sf}, q_{sk}, q_{sh}, q_{nsh}, q_{nsk})$  is shown in Fig. 3(a).

Due to the plastic impact of the rigid links, the double support phase is regarded as instantaneous [10]. Thus, the walking of DURUS-R has only one continuous domain as the non-stance leg swings in the air and one discrete event when the non-stance foot hits the ground. We model it as a *single domain hybrid control system* as a special case of (5). The single domain  $\mathcal{D}_r$  and the guard  $S_r$  are shown in Fig. 4(a). The holonomic constraints of  $\mathcal{D}_r$  are the positions of the stance foot  $(p_x, p_z)$  and the guard condition is the height of the non-stance foot. The continuous and discrete dynamics are determined from (9) and (10), respectively.

Since the robot has four actuated joints, the following four virtual constraints are considered, with the actual outputs defined as

$$y_r^a(q) = [q_{sk} \quad q_{nsk} \quad q_{tor} \quad \delta m_{nsl}]^T, \quad (24)$$

where  $\delta m_{nsl}$  is the linearized non-stance slope [1], and the desired outputs defined as  $y_r^d(\tau(q), \alpha_r)$ , as shown in Fig. 3(b). Then our goal is to find a parameter set  $\alpha_r$  such that the system has HZD. We will use the formulation in (23) for this problem.

To seek an efficient walking gait, we define the cost function as the *mechanical cost of transport* of the gait:

$$J_r(w_r) = \frac{W(w_r)}{mgd(w_r)}, \quad (25)$$

where  $w_r$  is the set of optimization variables for the domain  $\mathcal{D}_r$ ,  $W$  is the total absolute mechanical work done by the actuators,  $m$  is the total mass of the robot,  $g$  is the acceleration due to gravity, and  $d$  is the distance traveled

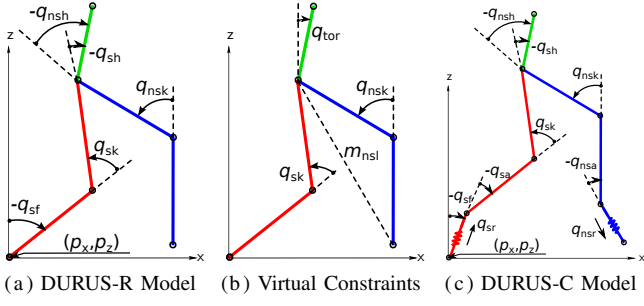


Fig. 3: Model configuration and outputs representation of DURUS-R and DURUS-C robot. DURUS-C has two extra spring links, one at the distal end of each leg.

during one step.  $W$  is the sum of the work done at each shooting grid,  $W_i(z_r^i, \alpha_r^i)$ , with

$$W_i(z_r^i, \alpha_r^i) = \int_{t_i}^{t_{i+1}} \sum_{j=1}^m |u_j^a(z_r^i, \alpha_r^i) \cdot \dot{q}_j^a(z_r^i, \alpha_r^i)| dt, \quad (26)$$

for  $i \in \{0, 1, \dots, n-1\}$ , where  $m$  is the number of actuated joints, and  $\dot{q}_j^a$  and  $u_j^a$  are the velocity and the actuator torque of the actuated joint  $j$ , computed from (20) and (14) respectively.

The following path constraints are considered:

- actuator torque limits,
- joint velocity limits,
- joint angle ranges,
- non-stance foot height clearance, and
- torso angle range.

The guard constraint is directly determined from the hybrid system definition of the robot. Additionally, two other constraints are considered:

- stability constraints of the zero dynamics periodic orbit: according to [22, p. 129], the stability condition of the two-dimensional hybrid zero dynamics can be explicitly examined without computing the Poincaré map, and
- an equality constraint time duration of continuous domain  $T_r^I$ : if the stability constraints are satisfied, the time duration of the two-dimensional zero dynamics can be explicitly solved, see [22, p. 131].

Finally the formulated optimization problem is implemented using the MATLAB function `fmincon`. The number of grids is chosen to be 20 in this paper, and the optimization algorithm is set to use its interior point method. The initial guess of the parameters  $\alpha$  is determined by fitting the human walking data introduced in [4]. Due to the complexity of system dynamics, the numerical Jacobian of the cost function and constraints are considered in the optimization problem instead of analytic Jacobian. The proposed optimization method in (23) converges as fast as the formulation in (1) in this case of two dimensional hybrid zero dynamics, but more reliably regardless of bad initial guesses.

### B. DURUS-C Model and Optimization

DURUS-C is a 3D-capable, humanoid bipedal robot that is still under development. In this example, we are only

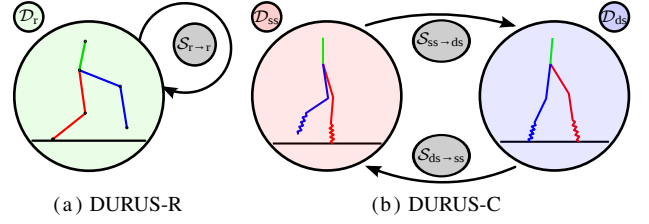


Fig. 4: The directed cycle of the hybrid control systems.

interested in the planar locomotion of this robot. One key improvement present in DURUS-C which differs from DURUS-R is a linear spring at the end of each leg. The compliance provided by the linear springs is designed to absorb energy at impact and reduce the energy loss so that more efficient locomotion can be achieved. The design of the compliant legs is inspired by the Spring-Loaded Inverted Pendulum model (SLIP). The SLIP model is widely used as a low-dimensional representation of bipedal locomotion to generate efficient behaviors due to the presence of compliance [5], [8].

The configuration  $q = (p_x, p_z, q_{sf}, q_{sr}, q_{sa}, q_{sk}, q_{sh}, q_{nsh}, q_{nsk}, q_{nsa}, q_{nsr})$  of the robot is shown in Fig. 3(c), where  $q_{sr}$  and  $q_{nsr}$  represent the deflections of the springs. Due to the existence of the springs, the stance foot will not leave the ground immediately after the non-stance foot hits the ground. Therefore, the walking of DURUS-C has two continuous domains: the *double support* domain  $\mathcal{D}_{ds}$ , where both feet are on the ground, and the *single support* domain  $\mathcal{D}_{ss}$ , where the non-stance leg swings in the air, as shown in Fig. 4(b).

The transition  $\mathcal{D}_{ss} \rightarrow \mathcal{D}_{ds}$  occurs when the non-stance foot hits the ground, and the transition  $\mathcal{D}_{ds} \rightarrow \mathcal{D}_{ss}$  occurs when non-stance spring reaches its rest length. Note that there will be a coordinate change after the foot hits the ground. The continuous and the discrete dynamics are computed according to (10) and (6), respectively. Note that spring dynamics, with stiffness  $k$  and damping  $b$ , are included in  $H(q, \dot{q})$  from (6) as  $H(q, \dot{q}) = C(q, \dot{q})\dot{q} + G(q) + B_s(kq + b\dot{q})$ , where  $B_s$  is the distribution matrix for the spring forces.

The choice of virtual constraints for DURUS-C is very similar to what we have picked for DURUS-R. In addition to outputs defined in (24), two ankle joints,  $q_{sa}$  and  $q_{nsa}$ , are also considered due to the fact that ankle joints are actuated in DURUS-C. Moreover,  $\delta m_{nsl}$  is omitted during the *double support* domain due to the fact that both legs are constrained on the ground so that the output  $\delta m_{nsl}$  which represents the forward motion of swing leg becomes redundant. Thus, we define the following outputs:

$$y_{ss}^a(q) = [q_{sk} \ q_{nsk} \ q_{tor} \ q_{sa} \ q_{nsa} \ \delta m_{nsl}]^T, \quad (27)$$

$$y_{ds}^a(q) = [q_{sk} \ q_{nsk} \ q_{tor} \ q_{sa} \ q_{nsa}]^T. \quad (28)$$

**Remark 1:** To have a square system, i.e., the inputs and the outputs have the same dimension, we assume that there are only five actuated joints in the system during the *double support* domain of DURUS-C walking by considering one of the originally actuated joints as passive. We pick the non-stance hip joint as the passive joint, since all outputs defined

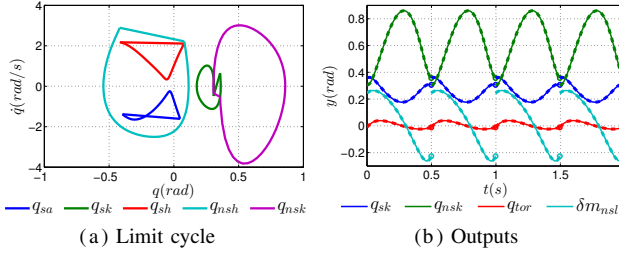


Fig. 5: Simulation result of stable periodic walking gait of DURUR-R.

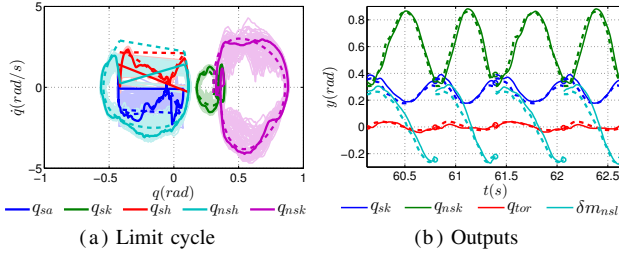


Fig. 6: Experimental result of stable periodic walking gait of DURUR-R.

in *double support* are not directly related to this joint.

The same cost function is used to generate an efficient and stable periodic gait through the HZD based multiple shooting optimization for DURUS-C. Since the time duration of  $\mathcal{D}_{ds}$  is much shorter than that of  $\mathcal{D}_{ss}$ , we set the shooting grids for the two domains to be 10 and 20, respectively.

The same path and guard constraints are imposed for the optimization of DURUS-C, as well. However, in the case of a high dimension zero dynamics model, i.e., more than two, the stability condition and time-to-impact constraints can not be explicitly computed. Thus, the stability of the resulting hybrid zero dynamics is checked off-line after the optimization by numerically solving for the fixed point of the Poincaré map of the zero dynamics. To obtain a stable gait, the maximum absolute value of all eigenvalues of the Jacobian of the Poincaré map should be less than one [16].

Since the mechanical structure of DURUS-C is inspired by the SLIP model, the initial guess of the parameter set is determined from the stable walking gait of the SLIP model. A similar approach can be found in [12]. Even with these raw fitted data as the initial guesses, the proposed optimization converges reliably. Moreover, though it has a higher dimension of zero dynamics, the DURUS-C optimization reaches to an optimal solution as fast as the case of DURUS-R.

## V. SIMULATION AND EXPERIMENTAL RESULTS

This section presents simulation results of stable periodic gaits generated from the HZD based multiple shooting optimization for DURUS-R and DURUS-C, and the experimental results of the DURUS-R gait.

### A. Simulation and Experimental Results of DURUS-R

Here, we describe a simulation of stable periodic walking gait for DURUS-R. In the simulation, the robot starts from

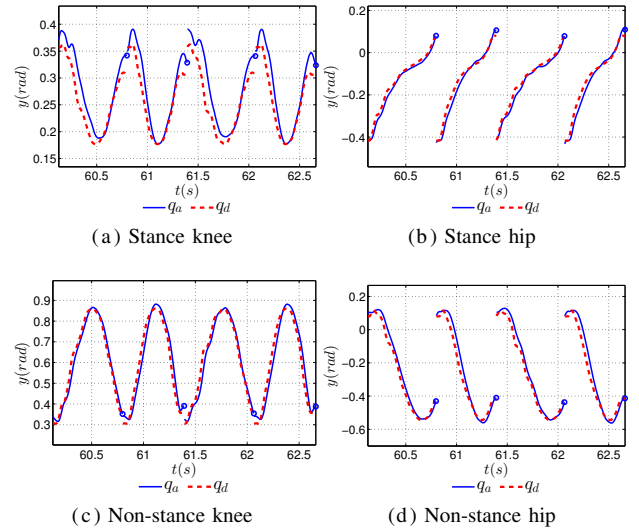


Fig. 7: Joint angles tracking performance of DURUR-R.

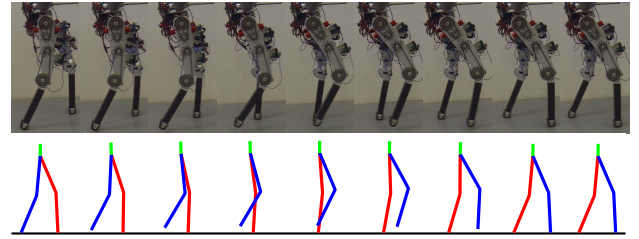


Fig. 8: The walking gait snapshot comparison of the simulation and experimental results with DURUS-R over one step.

the fixed point on the guard and is controlled by the feedback linearization controller defined in (14). The parameters  $\alpha$  are produced from the HZD based multiple shooting optimization and  $\varepsilon = 10$  is set as the control gain. The phase portraits of the robot joints in Fig. 5(a) show the resulting stable periodic orbit of the full order system. The maximum magnitude of eigenvalues of the full order system Poincaré map is 0.6461, which further proves the stability of the walking gait. Fig. 5(b) shows the tracking performance of the proposed controller.

The resulting walking gait is implemented experimentally on the hardware. The robot is supported by a freely-rotating four-bar linkage boom that restricts the motion of the robot to the sagittal plane while keeping the robot level with the ground. This boom design ensures that the boom neither holds the robot upward nor adds weight to the robot. The experiment was conducted by performing several trials under the same conditions. For each trial, the robot walks approximately 3 laps (45m) with no sign of failing before being stopped by the experimenter. Fig. 6(a) shows the phase portraits of the robot joints from the experimental data. The limit cycles deviate slightly from the corresponding limit cycles of the simulated gait, which are shown by dotted lines. The tracking of the outputs and joints are shown in Fig. 6(b) and Fig. 7 respectively. Fig. 8 shows

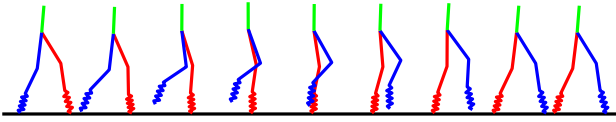


Fig. 9: The DURUS-C walking gait snapshot from the simulation.

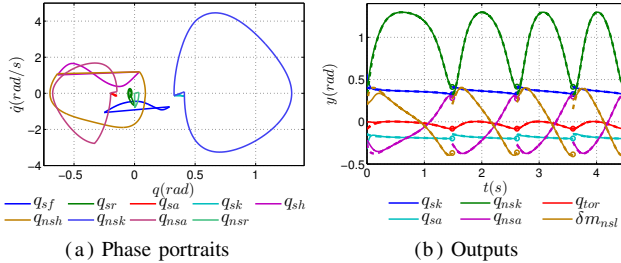


Fig. 10: Phase portraits of robot joints from the simulation of periodic stable walking gait on DURUS-C.

a stroboscopic comparison of the walking gait in simulation and experimentation during one step. The average cost of electrical transport for this gait is 0.75.

### B. Simulation Results of DURUS-C

Because DURUS-C is still being designed, only simulation results for the DURUS-C walking gait are presented. To show the periodic locomotion of the robot, Fig. 10(a) shows the limit cycles of the robot joints – including springs – from a simulation of a walking gait started from a fixed point on the periodic orbit by applying the feedback controller defined in (14). The maximum magnitude eigenvalue of the full order system Poincaré map is 0.5071 which shows the stability of the walking gait. Furthermore, another simulation started from a disturbed initial condition is performed to evaluate the convergence of the gait, as shown in Fig. 10(b). Fig. 9 shows the snapshots of the walking gait over one step.

## VI. CONCLUDING REMARKS

In summary, the proposed hybrid zero dynamics based multiple shooting method converges reliably and rapidly for two different robot models, DURUS-R and DURUS-C, even with bad initial guesses. Moreover, this method outperforms the single shooting method in the case of DURUS-C walking, where the latter often fails to converge to a feasible solution due to the multiple underactuated degrees of freedom of the robot. The end result is a stable, efficient gait for each robot, with a mechanical cost of transport of 0.3181 for DURUS-R and 0.0937 for DURUS-C in simulation, respectively. Finally, as was intended by design, the compliant leg of DURUS-C exhibited a smaller transport cost than its rigid-legged counterpart.

## REFERENCES

[1] A. D. Ames. Human-inspired control of bipedal walking robots. *IEEE Transactions on Automatic Control*, 59(5):1115–1130, May 2014.

[2] A. D. Ames, E. A. Cousineau, and M. J. Powell. Dynamically stable bipedal robotic walking with NAO via human-inspired hybrid zero dynamics. In *Proceedings of the 15th ACM international conference on Hybrid Systems: Computation and Control (HSCC)*, pages 135–144. ACM, 2012.

[3] A. D. Ames, K. Galloway, and J. W. Grizzle. Control Lyapunov functions and hybrid zero dynamics. In *2012 IEEE 51st Annual Conference on Decision and Control (CDC)*, pages 6837–6842, Dec 2012.

[4] A. D. Ames, R. Vasudevan, and R. Bajcsy. Human-data based cost of bipedal robotic walking. In *Proceedings of the 14th international conference on Hybrid Systems: Computation and Control (HSCC)*, pages 153–162. ACM, 2011.

[5] R. Blickhan. The spring-mass model for running and hopping. *Journal of Biomechanics*, 22(11):1217–1227, 1989.

[6] H. G. Bock and K. J. Plitt. *A multiple shooting algorithm for direct solution of optimal control problems*. Sonderforschungsbereich 72, Approximation u. Optimierung, Univ. Bonn, 1983.

[7] C. Chevallereau, G. Abba, Y. Aoustin, F. Plestan, E. R. Westervelt, C. C. De Wit, and J.W. Grizzle. RABBIT: A testbed for advanced control theory. *IEEE Control Systems Magazine*, 23(5):57–79, Oct 2003.

[8] S. Collins, A. Ruina, R. Tedrake, and M. Wisse. Efficient bipedal robots based on passive-dynamic walkers. *Science*, 307(5712):1082–1085, 2005.

[9] M. Diehl, H. G. Bock, H. Diedam, and P-B Wieber. Fast direct multiple shooting algorithms for optimal robot control. In *Fast Motions in Biomechanics and Robotics*, pages 65–93. Springer, 2006.

[10] J. W. Grizzle, C. Chevallereau, R. W. Sinnet, and A. D. Ames. Models, feedback control, and open problems of 3D bipedal robotic walking. *Automatica*, 50(8):1955 – 1988, 2014.

[11] J. Guckenheimer and S. Johnson. Planar hybrid systems. In *Hybrid Systems II*, volume 999 of *Lecture Notes in Computer Science*, pages 202–225. Springer Berlin Heidelberg, 1995.

[12] A. Hereid, S. Kolathaya, M. S. Jones, J. Van Why, J. W. Hurst, and A. D. Ames. Dynamic multi-domain bipedal walking with ATRIAS through slip based human-inspired control. In *Proceedings of the 17th International Conference on Hybrid Systems: Computation and Control (HSCC)*, pages 263–272. ACM, 2014.

[13] Y. Hurmuzlu and D. B. Marghitu. Rigid body collisions of planar kinematic chains with multiple contact points. *The International Journal of Robotics Research*, 13(1):82–92, 1994.

[14] Dieter Kraft. On converting optimal control problems into nonlinear programming problems. In *Computational Mathematical Programming*, pages 261–280. Springer, 1985.

[15] B. Morris and J.W. Grizzle. Hybrid invariant manifolds in systems with impulse effects with application to periodic locomotion in bipedal robots. *IEEE Transactions on Automatic Control*, 54(8):1751–1764, Aug 2009.

[16] T. S. Parker and L. O. Chua. *Practical numerical algorithms for chaotic systems*. Springer-Verlag, New York, 1989.

[17] A. Ramezani, J. W. Hurst, K. A. Hamed, and J. W. Grizzle. Performance analysis and feedback control of ATRIAS, A three-dimensional bipedal robot. *Journal of Dynamic Systems Measurement and Control*, 136(2), Mar 2014.

[18] A. V. Rao. A survey of numerical methods for optimal control. *Advances in the Astronautical Sciences*, 135(1):497–528, 2009.

[19] R. W. Sinnet and A. D. Ames. 2D bipedal walking with knees and feet: A hybrid control approach. In *Proceedings of the Joint 48th IEEE Conference on Decision and Control and 28th Chinese Control Conference (CDC/CCC)*, pages 3200–3207, Shanghai, December 2009.

[20] K. Sreenath, H. Park, I. Poulakakis, and J. W. Grizzle. A compliant hybrid zero dynamics controller for stable, efficient and fast bipedal walking on MABEL. *The International Journal of Robotics Research*, 30(9):1170–1193, 2011.

[21] O. Von Stryk. *Numerical solution of optimal control problems by direct collocation*. Springer, 1993.

[22] E. R. Westervelt, J. W. Grizzle, C. Chevallereau, J. H. Choi, and B. Morris. *Feedback control of dynamic bipedal robot locomotion*. CRC press Boca Raton, 2007.

[23] E. R. Westervelt, B. Morris, and K. D. Farrell. Analysis results and tools for the control of planar bipedal gaits using hybrid zero dynamics. *Autonomous Robots*, 23(2):131–145, 2007.